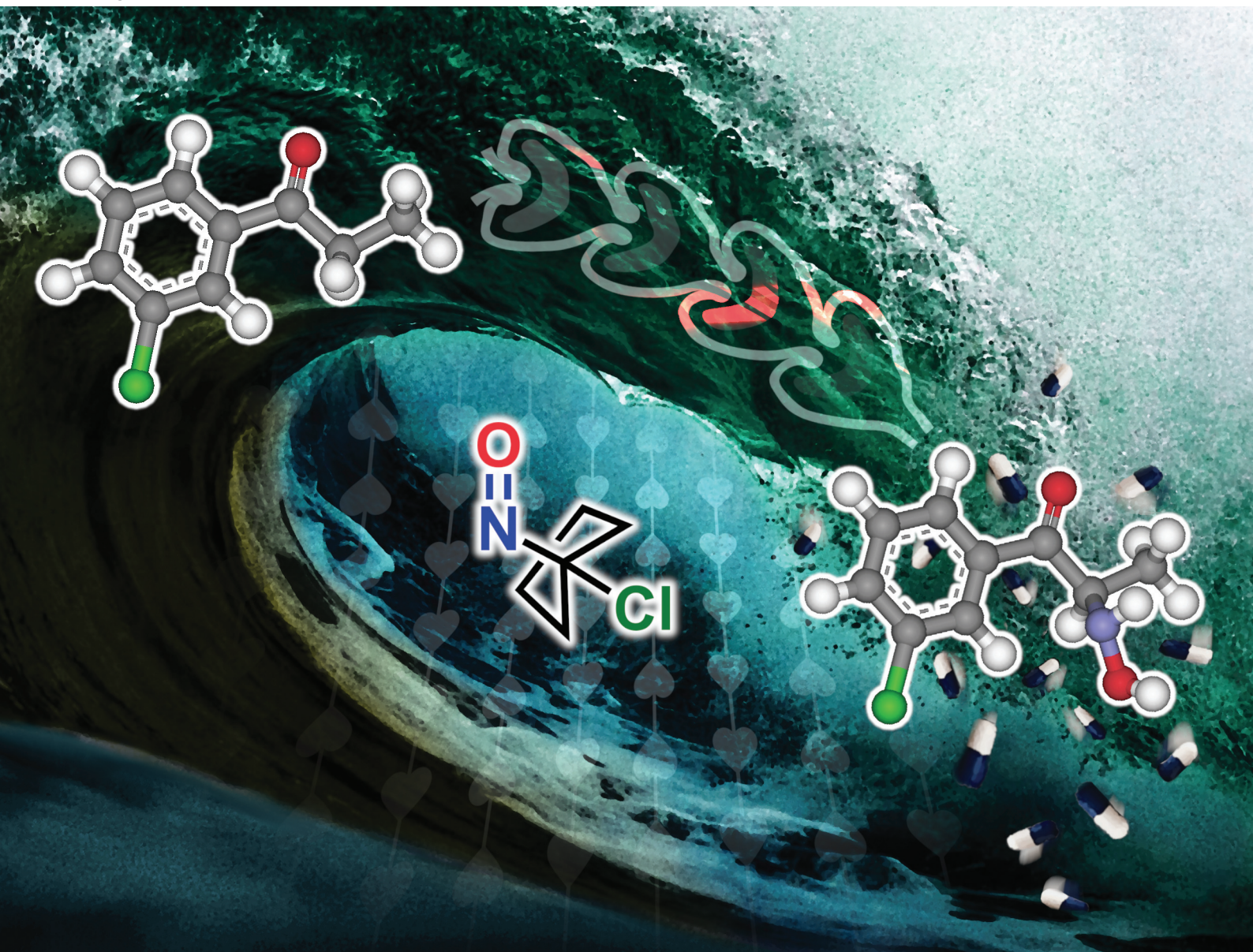


Green Chemistry

Cutting-edge research for a greener sustainable future

rsc.li/greenchem



ISSN 1463-9262

PAPER

Jean-Christophe M. Monbaliu *et al.*
A modular, low footprint and scalable flow platform for the
expeditious α -aminohydroxylation of enolizable ketones



Cite this: *Green Chem.*, 2021, **23**, 2336

A modular, low footprint and scalable flow platform for the expedient α -aminohydroxylation of enolizable ketones†

Victor-Emmanuel H. Kassin,^a Romain Morodo,^a Thomas Toupy,^a Isaline Jacquemin,^a Kristof Van Hecke,^b Raphaël Robiette^c and Jean-Christophe M. Monbaliu^{b,*a}

The unique reactivity profile of α -chloronitroso derivatives is expressed to its fullest potential through the development of an integrated, modular and scalable continuous flow process for the electrophilic α -aminohydroxylation of various enolizable ketones. Flow conditions contribute to mitigating the high reactivity and toxicity of α -chloronitroso derivatives and provide an efficient, versatile and safe protocol for the α -aminohydroxylation of ketones with a minimal footprint. Fundamental aspects of the α -aminohydroxylation process were computed by DFT and further supported the experimental observations, hence leading to the unprecedented α -chloronitroso-based α -aminohydroxylation of primary, secondary and tertiary substrates. Recycling of the carbon backbone of the α -chloronitroso derivatives provides a high atom economy for the preparation of value-added molecules. This work showcases α -chloronitroso derivatives as economic and efficient vehicles for transferring electrophilic synthons of hydroxylamine toward nucleophilic enolates. A representative range of precursors and analogs of pharmaceutical active ingredients, including WHO essentials and drugs in shortage (such as epinephrine and ketamine), are prepared within minutes according to a fully concatenated process. The process features sequential modules with distinct unit operations including chemical transformations and multiple in-line extractions. The process relies on an upstream chemical Generator that manages the preparation of α -chloronitroso derivatives and that feeds downstream a series of α -aminohydroxylation modules. The setup is amenable to the addition of libraries of compounds for feeding upstream the process of discovery in medicinal chemistry and is transposable to pilot scale. Several layers of in-line analytical procedures are featured to improve process control and safety.

Received 28th December 2020,

Accepted 1st February 2021

DOI: 10.1039/d0gc04395h

rsc.li/greenchem

Introduction

Nitrogen, which is the fourth element in abundance in biogenic material, is ubiquitous in biomolecules from peptides to neurotransmitters. Nitrogen-containing organics are therefore privileged scaffolds for active pharmaceutical ingredients (APIs), among which β -amino alcohols and α -aminoketones are abundantly represented (Fig. 1). The development of amin-

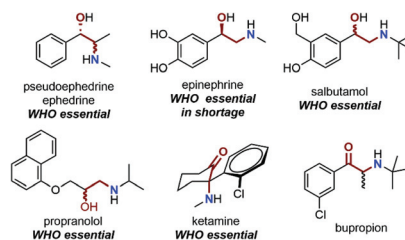


Fig. 1 Representative examples of β -amino alcohol and α -aminoketone APIs and biologically active compounds. Pseudoephedrine and ephedrine are listed as WHO essential drugs,²⁰ and are mainly used as sympathomimetic sinus decongestant and stimulant, respectively. Epinephrine, also known as adrenalin, is a neurotransmitter and a WHO essential drug currently in shortage.^{20–22} Salbutamol is a β -amino alcohol active pharmaceutical listed as essential by WHO used mainly for the treatment of asthma.²⁰ Propranolol, another WHO essential β -amino alcohol, is a common β -blocker medication for treating cardiovascular conditions.²⁰ Ketamine and bupropion are two representative α -aminoketones prescribed mainly for treating severe depression. Ketamine is listed as WHO essential.²⁰

^aCenter for Integrated Technology and Organic Synthesis, MolSys Research Unit, University of Liège, B-4000 Liège (Sart Tilman), Belgium.

E-mail: jc.monbaliu@uliege.be; <http://www.citos.uliege.be>

^bXStruct, Department of Chemistry, Ghent University, Krijgslaan 281-S3, B-9000 Ghent, Belgium

^cInstitute of Condensed Matter and Nanosciences, Université catholique de Louvain, Place Louis Pasteur 1, 1348 Louvain-la-Neuve, Belgium

†Electronic supplementary information (ESI) available: Fluidic components, experimental procedures, details of the fluidic setup and procedures (micro- and mesoscale), off-line analysis with structural assignments (NMR and X-ray diffraction) and computations. CCDC 2046130–2046136. For ESI and crystallographic data in CIF or other electronic format see DOI: 10.1039/d0gc04395h

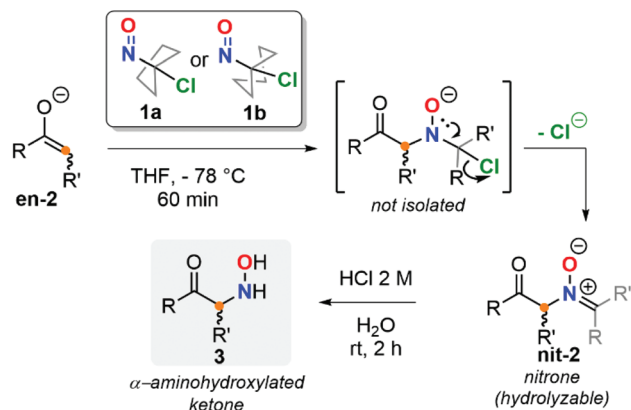


Fig. 2 Illustration and detailed mechanism for the electrophilic amination of enolizable ketone substrates (also known as the nitroso aldol reaction) with α -chloronitroso derivatives **1a,b** showing the formation of an intermediate nitronium **nit-2** and its subsequent solvolysis toward a free α -aminohydroxylated ketone **3**.

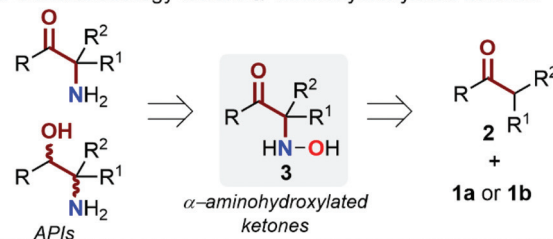
ation procedures starting from common, widely available substrates therefore stimulates lots of research efforts.^{1–4} Typical amination procedures exploit the inherent nucleophilic nature of nitrogen for its insertion on activated electrophilic substrates.^{5–11} Alternative methods relying on the umpolung of nitrogen, known as electrophilic aminations, are also abundantly documented in the literature.^{12–19}

A variety of electrophilic amination reagents have been reported, among which azodicarboxylates,^{23–29} diazoesters,³⁰ haloamines,^{30–32} hydroxylamines and derivatives,^{30,32–35} oxaziridines,^{11,36} as well as nitroso derivatives are documented (Fig. 2). The latter class counts several subclasses that share a common electrophilic N=O moiety that is modulated through specific structural features. Nitroso derivatives are versatile chemicals that have been used for formal amination reactions starting from various substrates mainly through hetero Diels–Alder,^{37–44} ene^{40,45–48} and *O*- or *N*-nitroso aldol reactions.^{48–51}

Among nitroso derivatives, α -chloronitroso (also known as 1-chloro-1-nitroso or *gem*-chloronitroso) derivatives such as 1-chloro-1-nitrosocyclopentane **1a** and 1-chloro-1-nitrosocyclohexane **1b** (Fig. 2) are underrepresented in the literature, despite their inherent appealing reactivity profile. Alike other nitroso derivatives, they can be involved in hetero Diels–Alder^{52–56} and nitroso aldol reactions,^{57–64} yet unlike other nitroso species, the carbon backbone is readily released through solvolysis, hence avoiding tedious or wasteful deprotection protocols to release the aminohydroxyl function (Fig. 2). The mechanism, which is illustrated in Fig. 2 for a nitroso-aldol reaction (*i.e.* the electrophilic amination of an enolizable substrate), involves the formation of an intermediate nitronium **nit-2**, which solvolyzes in lower alcohols or in acidic water. The carbon backbone is released as a ketal (solvolysis in lower alcohols) or as a ketone (acidic hydrolysis). The α -aminohydroxylated ketones obtained accordingly are poten-

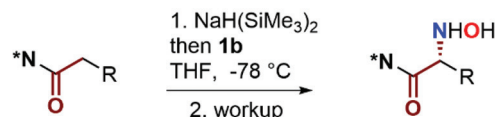
tially versatile intermediates for rapidly accessing various β -amino alcohol and α -aminoketone scaffolds, which are commonly encountered in pharmaceuticals and other biologically active molecules (Fig. 3a). In this context, Oppolzer's seminal work for electrophilic aminations of enolizable carbonyls with α -chloronitroso compounds (Fig. 3b) is still a landmark.^{57–62} Oppolzer's amination was also amenable to stereoselective protocols, either using chiral auxiliaries on the substrate or chiral nitroso compounds.

a. General strategy toward α -aminohydroxylated ketones



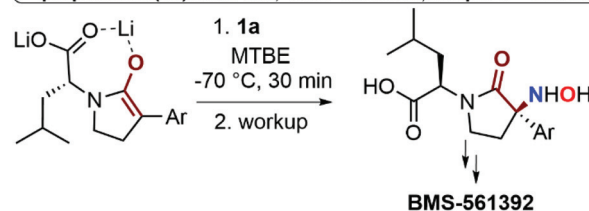
b. Lab scale batch electrophilic amination on 2^{ary} and 3^{ary} substrates (Oppolzer *et al.*)

preparation and use (1b): < 5 mmol; **scope:** 2, 3^{ary} amides, ketones



c. Large scale batch electrophilic amination on 3^{ary} substrates (Magnus *et al.*)

preparation (1a): 6.06 mol, **use:** 153 mmol; **scope:** 3^{ary} lactam



d. This work: continuous flow electrophilic amination on 1^{ary}, 2^{ary} and 3^{ary} substrates

preparation and use (1a): scale-independent **scope:** 1-3^{ary} ketones

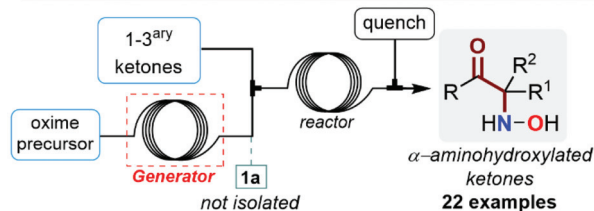


Fig. 3 (a) α -Aminohydroxylated ketones obtained from the reaction of enolizable ketones and α -chloronitroso **1a,b** are versatile intermediates for rapidly accessing various β -amino alcohol and α -aminoketone scaffolds. (b) Oppolzer's α -aminohydroxylation on chiral amides (N^* = (2*R*)- or (2*S*)-bornane-10,2-sultam) with **1b**.^{57–62} (c) Large scale preparation of anti-inflammatory drug candidate **BMS-561392** involving a key electrophilic α -aminohydroxylation using **1a**.⁶⁵ (d) This work significantly extends the scope of the α -aminohydroxylation with α -chloronitroso derivatives such as **1a** to primary, secondary and tertiary enolizable substrates under scalable flow conditions.

There is only one example in the recent literature that illustrates a large-scale batch application relying on compound **1a** (Fig. 3c). Compound **1a** was used to install a quaternary center on a key intermediate toward anti-inflammatory compound **BMS-561392** (Fig. 3c).⁶⁵ This protocol was developed at Bristol-Myers Squibb and required labor- and energy-intensive conditions. Besides, the authors indicated that “*data substantiated that the aminating agent 1-chloro-1-nitrosocyclopentane was not safe to use*”⁶⁵ on such a preparative scale. The unstable and explosive nature of **1a** imposed $-78\text{ }^{\circ}\text{C}$ for the effective amination of a leucine-derived enolizable amide.⁶⁵

With increasingly restrictive legislations both at the R&D and commercial scales, the use of reactive and potentially hazardous chemicals has become limiting if not impossible with conventional batch reactors. The concept of chemical generators under continuous flow conditions has been extensively documented by Kappe,^{66–72} hence providing a robust answer for exploiting reactive intermediates yet benefiting from all the safety and process advantages of continuous flow operation. A continuous flow chemical generator actually relies on stable and widely available precursors and on the concatenation of upstream operations aiming at the preparation of unstable, toxic or reactive chemicals, which are next immediately consumed within downstream operations (Fig. 3d). Such a scheme alleviates the safety concerns of handling and stockpiling reactive chemicals. Building upon our expertise in developing continuous flow processes^{73–77} and the handling of nitroso species,^{37,38,78,79} a solution was sought for exploiting, under safe conditions, the unique reactivity of α -chloronitroso derivatives at its fullest.

We describe herein the development of a low footprint, modular, safe and scalable continuous flow process for the electrophilic α -aminohydroxylation of various enolizable ketones (Fig. 3d). Building upon the highly reactive nature of α -chloronitroso derivatives, this flow process revisits Oppolzer’s classical procedure for the α -aminohydroxylation of enolizable ketones and is amenable to either R&D or production scales. Flow conditions contribute to mitigate the high reactivity and toxicity of α -chloronitroso derivatives. The flow process features two chemical generators connected in series: (a) Generator I for the preparation of strong organic oxidizer *tert*-butyl hypochlorite (**tBuOCl**) from common and stable precursors; (b) and Generator II for the generation of α -chloronitroso derivatives from stable and widely available oximes and **tBuOCl** (from Generator I). Generator II then feeds a series of fluidic modules for the α -aminohydroxylation of enolates with α -chloronitroso derivatives, producing a variety of racemic α -aminohydroxylated ketone hydrochlorides in water. Each fluidic element also includes additional operations such as extraction, quench, hydrolysis and in-line analysis, hence providing a complex, fully integrated process. Generators I and II alleviate the storage and handling of two toxic and unstable chemicals, *i.e.* **tBuOCl** and α -chloronitroso derivatives, hence drastically improving the safety features of the process. The flow proto-

col was first validated on a series of model primary and secondary enolizable ketone derivatives, and then broadened to other enolizable ketones, including tertiary substrates. The protocol is versatile and also features options for controlling the α -aminohydroxylation of unsymmetrical enolizable ketones under thermodynamic and kinetic conditions. Last, but not least, this protocol also enables the unprecedented α -aminohydroxylation of primary enolizable ketones, which is very challenging to achieve under conventional batch conditions. A DFT study indicated that the α -aminohydroxylation step is diffusion-controlled and supported the experimental observations. Besides the wide functional diversity obtained through this method, the by-product of the reaction, *i.e.* the carbon backbone of the α -chloronitroso derivative (*i.e.* cyclopentanone for 1-chloro-1-nitrosocyclopentane **1a**) is recyclable and readily transformed with hydroxylamine hydrochloride into the corresponding oxime for feeding Generator II, hence showcasing α -chloronitroso derivatives as economic and efficient vehicles for transferring electrophilic synthons of hydroxylamine toward nucleophilic enolates.

Experimental section

General information

Conversion and yield were determined by HPLC/DAD or by high field ^1H NMR spectroscopy. Structural identity was confirmed by ^1H and ^{13}C NMR spectroscopy (400 MHz Bruker Avance spectrometer) in CDCl_3 , CD_3OD or D_2O and by X-ray diffraction on single crystals of compounds *rac*-**3g-HCl**, **3q**, **3r**, **3t-HCl**, **3u**, **5**, **6** and **7** (CCDC 2046130–2046136†). Compounds **6** and **7** are described in the ESI only, see sections 2.3, 2.5 and 2.6†. The chemical shifts are reported in ppm relative to TMS as an internal standard or to the solvent residual peak. Solvents (diethyl ether, absolute ethanol, methanol, hexanes, petroleum ether (40–60) and ethyl acetate) were used as received, unless otherwise stated. Tetrahydrofuran (THF) and methyl *tert*-butyl ether (MTBE) were distilled over Na/benzophenone. Sodium hypochlorite pentahydrate, *tert*-butanol, glacial acetic acid, acetoxime, 2-butanone oxime, cyclopentanone oxime, cyclohexanone oxime, cycloheptanone oxime, (–)-menthone, (+)-camphor, acetophenone, propiophenone, 4′-methylpropiophenone, 3′-chloro-propiophenone, 4′-chloro-propiophenone, 4′-fluoropropiophenone, 4′-(trifluoromethyl)-propiophenone, 2′-(trifluoromethyl)-propiophenone, 3′-(trifluoromethyl)-propiophenone, 3′-nitropropiophenone, 4′-methoxy-propiophenone, valerophenone, octanophenone, 1-(2-thienyl)-1-propanone, 1,3-diphenylpropan-1-one, 1-(benzo[*d*][1,3]-dioxol-5-yl)propan-1-one, isobutyrophenone, 1,2-diphenylethan-1-one, cyclobutyl phenyl ketone, cyclopentyl phenyl ketone, 2-chlorophenyl cyclopentyl ketone, cyclohexyl phenyl ketone, 2-phenylcyclohexanone, lithium bis(trimethylsilyl)amide (*ca.* 26% in THF), hydroxylamine hydrochloride, sodium acetate trihydrate, pyridine, zinc chloride (*ca.* 25% in THF), sodium bicarbonate, potassium *tert*-butoxide, potassium hydroxide,

sodium borohydride and zinc dust, calcium chloride, potassium iodide, sodium thiosulfate, potassium bichromate were obtained from commercial sources and used as received.

Experimental setup

Microfluidic setups. Microfluidic reactors consisted of modular continuous flow assemblies constructed from PFA tubing (1.58 mm outer diameter, 750 μm internal diameter) equipped with PEEK/ETFE connectors and ferrules (IDEX/Upchurch Scientific). Feed and collection lines consisted of PFA or PEEK tubing (1.58 mm outer diameter, 750 μm internal diameter) equipped with PEEK/ETFE connectors and ferrules (IDEX/Upchurch Scientific). Liquid feeds were handled with high force Chemyx Fusion 6000 syringe pumps equipped with SS syringes and DuPont Kalrez O-rings or with HPLC pumps (ThalesNano micro HPLC). The coil reactors were thermoregulated with a Heidolph MR Hei-Tec equipped with a Pt-1000 temperature sensor. Downstream pressure was regulated with back pressure regulators from Zaiput Flow Technologies (BPR-10) or from IDEX/Upchurch Scientific. Liquid-liquid extraction was carried out with a Zaiput Flow Technologies membrane separator (SEP-10, equipped with a 1 μm pore hydrophobic membrane).

Mesofluidic setup – lab scale. Lab scale mesofluidic experiments were carried out in a Corning® Advanced-Flow™ Low Flow Reactor (0.5 mL internal volume glass fluidic modules). Feed and collection lines consisted of PFA tubing (1/8" o.d.) equipped with PFA or SS Swagelok connectors and ferrules. Liquid feeds were handled with FLOM or ThalesNano micro HPLC pumps. The reactor was maintained at reaction temperature with a LAUDA Integral XT 280 thermostat and a LAUDA Proline RP845. Downstream pressure was regulated with a back pressure regulator from Zaiput Flow Technologies (BPR-10 or BPR-1000). Downstream membrane separation relied on a membrane separator from Zaiput Flow Technologies (SEP-10, equipped with a 1 μm pore hydrophobic membrane). In-line analysis was performed on an in-line IR (FlowIR™ from Mettler-Toledo equipped with a DTGS detector using HappGenzel apodization, a Silicon probe connected *via* a FlowIR™ sensor and a high pressure heated 10 μL cell) or a benchtop NMR (43 MHz Spinsolve™ ^1H NMR spectrometer from Magritek® equipped with a flow-through cell).

Mesofluidic setup – pilot scale. Mesofluidic experiments were carried out in a Corning® Advanced-Flow™ G1 Reactor (8 mL internal volume glass fluidic modules for the preparation of **tBuOCl** and **1a,b**) or in a Corning® Advanced-Flow™ G1 SiC Reactor (8 mL internal volume silicon carbide fluidic modules for the preparation of *rac*-**3b** and *rac*-**3k**). Feed and collection lines consisted of PFA tubing (1/8" or 1/4" o.d.) equipped with PFA or SS Swagelok connectors and ferrules. Liquid feeds were handled with Corning® dosing lines (FUJI Technologies™ and HNP Mikrosysteme pumps). The reactor was maintained at reaction temperature with a LAUDA Integral XT 280 thermostat. Downstream pressure was regulated with a back pressure regulator from Zaiput Flow Technologies

(BPR-1000). Downstream membrane separation relied on a membrane separator from Zaiput Flow Technologies (SEP-200, equipped with a 1 μm pore hydrophobic membrane). In-line analysis was optionally performed with an IR spectrometer (FlowIR™ from Mettler-Toledo equipped with a DTGS detector using HappGenzel apodization, a Silicon probe connected *via* a FlowIR™ sensor and a high pressure heated 50 μL cell) or a benchtop NMR (43 MHz Spinsolve™ ^1H NMR spectrometer from Magritek® equipped with a flow-through cell).

Computational study

Calculations were carried out using the Jaguar 8.5 program package.⁸⁰ Geometry optimizations were performed at the B3LYP-D3/6-31+G* level of theory. Solvent effects were modelled by using the polarizable continuum-Poisson method as incorporated in Jaguar, using the parameters for MTBE, *i.e.*, a dielectric constant of 2.6, and a solvent probe radius of 2.42 Å. Full calculation of vibrational frequencies was performed at the B3LYP-D3/6-31+G* level using ultrafine grids to characterize the stationary points (local minima no imaginary frequencies and transition states one imaginary frequency) and to obtain Gibbs free energy correction. The calculated reaction profile was verified for each transition state by following the intrinsic reaction coordinate (IRC). In Jaguar, the translational partition function is computed for ideal gas standard conditions, corresponding to a pressure of 1 atm at 298.15 K. For solution reactions, the standard condition is instead 1 mol L⁻¹. Accordingly, the free energy value computed in Jaguar was corrected by a concentration term, equal to $RT \ln(V_{\text{mol_gas}}/1 \text{ atm}/V_{\text{mol}}/1 \text{ M})$, *i.e.*, 1.89 kcal mol⁻¹ at 298.15 K. Electronic energies were computed at the B3LYP-D3/6-311+G** level whereas solvation energies were obtained at the B3LYP-D3/6-31+G*(MTBE). A systematic attempt to locate all possible local minima (at the B3LYP-D3/6-31+G* level) was made, with the data presented referring to the lowest energy form.

Typical runs

CAUTION: Reactor setups involving **tBuOCl**, 1-chloro-1-nitrosocyclopentane (**1a**) and 1-chloro-1-nitrosocyclohexane (**1b**) were covered in thin foil to prevent light exposure. **tBuOCl**, **1a** and **1b** are reactive and unstable species with a pungent smell that decompose under heat or UV irradiation. They must be handled with great care under a fume hood in the absence of direct light.^{81,82} If necessary, storage over CaCl_2 at -8°C in a brown glass bottle is recommended. Careful neutralization of **tBuOCl** over thioanisole⁸³ and of **1a,b** over triphenylphosphine⁸⁴ is strongly advised before disposal.

Concatenated continuous flow preparation of 1-chloro-1-nitrosocyclopentane 1a (lab scale). The feed solution of sodium hypochlorite (1.5 M in water) and an aqueous solution of acetic acid and *tert*-butanol (1 M, 1 : 1) were both injected at 0.1 mL min⁻¹ and reacted in a PFA capillary coil for 5 min at 25 °C. MTBE was injected downstream (0.2 mL min⁻¹) and **tBuOCl** was extracted through a short column loaded with glass beads ($\phi = 0.1$ mm). After liquid-liquid separation through a hydrophobic membrane separator, the organic

permeate was mixed with a solution of cyclopentanone oxime **4a** (1 M in MTBE, 0.2 mL min⁻¹) through a PEEK T-mixer and reacted in a PFA capillary coil (2 mL internal volume, 5 min residence time) at 25 °C. The reactor effluent was passed through an in-line IR spectrometer for reaction monitoring and then quenched with a stream of aqueous sodium carbonate (10 wt%, 0.2 mL min⁻¹) under 5 bar of counterpressure. Downstream liquid-liquid separation through a hydrophobic membrane separator yielded 1-chloro-1-nitrosocyclopentane (**1a**) in MTBE (0.5 M). The aqueous retentate was redirected to a waste container.

Concatenated continuous flow preparation of 1-chloro-1-nitrosocyclopentane 1a (mesofluidic scale). An aqueous solution containing *tert*-butanol (1 M) and acetic acid (1 M) was reacted with another aqueous solution of sodium hypochlorite (2.25 M) in a Corning® Advanced-Flow™ Low Flow Reactor (4 fluidic modules connected in series, 2.0 mL total internal volume, operated at 25 °C). MTBE was subsequently injected into the system and two additional fluidic modules were used for the extraction (1 mL total internal volume, operated at 25 °C). The resulting biphasic stream was processed through a hydrophobic membrane separator. The organic permeate (*t*BuOCl, 1 M in MTBE) was next mixed with a solution containing cyclopentanone oxime (**4a**, 1 M in MTBE) and reacted into a second reactor consisting of 3 fluidic modules connected in series (1.5 mL total internal volume, operated at 10 °C). The effluent was next passed through an in-line IR spectrometer for real-time monitoring under 5 bar of counterpressure. All pumps were set to 2 mL min⁻¹, affording an estimated residence time of 30 s for the preparation of *t*BuOCl and of 22.5 s for the preparation of **1a**.

Concatenated continuous flow preparation of 1-chloro-1-nitrosocyclopentane 1a (pilot⁸¹ scale). An aqueous solution containing *tert*-butanol (1 M) and acetic acid (1 M) was mixed with an aqueous solution of sodium hypochlorite (2.25 M) in a Corning® Advanced-Flow™ G1 Reactor (2 fluidic modules connected in series, 16 mL total internal volume, operated at 25 °C). MTBE was subsequently injected into the system and the extraction was carried out in an additional fluidic module (8 mL internal volume, operated at 25 °C). The resulting biphasic stream was processed into a membrane separator. The organic permeate (*t*BuOCl, 1 M in MTBE) was next mixed with a solution containing cyclopentanone oxime (**4a**, 1 M in MTBE) and reacted in an additional fluidic module (8 mL internal volume, operated at 10 °C). The effluent was next passed through an in-line IR spectrometer for real-time monitoring under 5 bar of counterpressure. The reactor effluent was neutralized in a collection tank containing a solution of triphenylphosphine (1 M in a 1:1 MTBE/MeOH mixture). All pumps were set to 15 mL min⁻¹, affording an estimated residence time of 36 s for the preparation of *t*BuOCl and of 18 s for the preparation of **1a**.

Neutralization of 1-chloro-1-nitrosocyclopentane 1a. CAUTION: the neutralization of **1a** is exothermic. To 5 mL of a stirred solution of **1a** (1 M, 5 mmol, 1 equiv.), 20 mL of a solution of triphenylphosphine (0.25 M, 5 mmol, 1 equiv.) in a

1:1 MTBE/MeOH mixture were added dropwise at room temperature. The mixture was left under intense stirring for 1 h to complete neutralization (the neutralization rate was measured through HPLC/DAD by monitoring the formation of triphenylphosphine oxide, see ESI, section 2.2.15†). Upon neutralization, the characteristic blue color of **1a** slowly faded away.

Concatenated continuous flow α -aminohydroxylation of propiophenone 2b. A feed solution of sodium hypochlorite (1.5 M) and an aqueous mixture of acetic acid and *tert*-butanol (1 M, 1:1) were both injected at 0.1 mL min⁻¹ through a PEEK T-mixer and reacted in a PFA capillary coil for 5 min at 25 °C. MTBE was injected downstream the reactor (0.2 mL min⁻¹) to extract *t*BuOCl through a short column loaded with glass beads ($\phi = 0.1$ mm). The biphasic mixture was next processed through a membrane separator. The aqueous retentate was redirected to a waste tank. The organic permeate (*t*BuOCl, 1 M in MTBE) was redirected toward a PEEK T-mixer where it was mixed with a stream of cyclopentanone oxime (**4a**, 1 M in MTBE, 0.2 mL min⁻¹). The resulting mixture was reacted in a PFA capillary coil (2 mL internal volume, 5 min residence time) at 25 °C. The reactor effluent was connected to an in-line IR spectrometer for reaction monitoring and then quenched with a stream of aqueous sodium carbonate (10 wt%, 0.2 mL min⁻¹). Downstream liquid-liquid separation through a hydrophobic membrane separator yielded 1-chloro-1-nitrosocyclopentane (**1a**) in MTBE (0.5 M). The organic permeate was passed through a short column loaded with molecular sieve (MS 3 Å) prior to further downstream processing. The upstream enolization reaction involved two pumps used to deliver a solution of propiophenone (**2b**, 0.5 M in dry THF) and LiHMDS (0.5 M in dry THF). Both pumps were set to 0.4 mL min⁻¹ and the resulting mixture was reacted in a PFA capillary coil (0.8 mL internal volume, 1 min residence time) at 0 °C. The reactor effluent from the enolization step was mixed with the stream of **1a** through a PEEK T-mixer and reacted in a PFA capillary coil (1.2 mL internal volume, 1 min residence time) at 0 °C. The reactor effluent was next mixed through a PEEK T-mixer with an aqueous solution of HCl (6 M) injected with a pump set at 0.4 mL min⁻¹. The mixture was reacted in a PFA capillary coil (1.6 mL internal volume, 1 min residence time) at 60 °C. The entire setup was operated under 5 bar of counterpressure. A final liquid-liquid membrane separator was inserted downstream and the aqueous retentate was collected at steady state, diluted with MeOH, and analyzed by HPLC/DAD (97% conv., 90% yield).

General continuous flow protocol for the α -aminohydroxylation of enolizable ketones 2a-u. The pumps used to deliver ketones **2a-u** (0.5 M in dry THF) and LiHMDS (0.5 M in dry THF) were both set to 0.1 mL min⁻¹. Both streams were mixed through a PEEK T-mixer. The mixture was reacted in a PFA capillary coil (0.2 mL internal volume, estimated 1 min residence time) at 0 °C. The reactor effluent was next mixed through a PEEK T-mixer with 1-chloro-1-nitrosocyclopentane (**1a**, 0.5 M in MTBE, 0.11 mL min⁻¹) and redirected toward a PFA capillary coil (0.31 mL internal volume, 1 min residence time) operated at 0 °C. The reactor effluent

was next mixed through a PEEK T-mixer with an aqueous solution of HCl (6 M) injected with a pump set to 0.3 mL min⁻¹. The mixture was reacted in PFA capillary coil (0.61 mL internal volume, 1 min residence time) at 60 °C. The entire setup was operated under 5 bar of counterpressure. A final liquid–liquid membrane separator was inserted downstream and the aqueous retentate was collected at steady state, diluted with MeOH, and analyzed by HPLC/DAD. Conversion and isolated yield: starting from acetophenone **2a** (**3a**, 70% conv., 62% yield), propiophenone **2b** (**3b**, 97% conv., 90% yield), 1-(*p*-tolyl)propan-1-one **2c** (**3c**, 96% conv., 88% yield), 1-(4-methoxyphenyl)propan-1-one **2d** (**3d**, 97% conv., 78% yield), 1-(benzo[*d*][1,3]dioxol-5-yl)propan-1-one **2e** (**3e**, 80% conv., 74% yield), 1-(4-chlorophenyl)propan-1-one **2f** (**3f**, 97% conv., 95% yield), 1-(4-(trifluoromethyl)phenyl)propan-1-one **2g** (**3g**, 79% conv., 73% yield), 1-(4-fluorophenyl)propan-1-one **2h** (**3h**, 91% conv., 86% yield), 1-(3-(trifluoromethyl)phenyl)propan-1-one **2i** (**3i**, 75% conv., 64% yield), 1-(3-nitrophenyl)propan-1-one **2j** (**3j**, 75% conv., 65% yield), 1-(3-chlorophenyl)propan-1-one **2k** (**3k**, 88% conv., 80% yield), 1-(2-(trifluoromethyl)phenyl)propan-1-one **2l** (**3l**, 77% conv., 49% yield), 1-(thiophen-2-yl)propan-1-one **2m** (**3m**, 93% conv., 60% yield), 1-phenylpentan-1-one **2n** (**3n**, 83% conv., 79% yield), 1-phenyloctan-1-one **2o** (**3o**, 76% conv., 72% yield), 1,3-diphenylpropan-1-one **2p** (**3p**, 89% conv., 74% yield), 2-methyl-1-phenylpropan-1-one **2q** (**3q**, 85% conv., 82% yield), cyclobutyl(phenyl)methanone **2r** (**3r**, 87% conv., 84% yield), cyclohexyl(phenyl)methanone **2s** (**3s**, 78% conv., 75% yield), cyclopentyl(phenyl)methanone **2t** (**3t**, 82% conv., 72% yield), (2-chlorophenyl)(cyclopentyl)methanone **2u** (**3u**, 98% conv., 80% yield).

Continuous flow protocol for the α -aminohydroxylation of ketone **2v under thermodynamic or kinetic conditions.** The pumps used to deliver 2-phenylcyclohexan-1-one (**2v**, 0.5 M in dry THF) and either LiHMDS (0.5 M in dry THF, kinetic conditions) or potassium *tert*-butoxide (0.5 M in dry THF, thermodynamic conditions) were both set to 0.1 mL min⁻¹. Both streams were mixed through a PEEK T-mixer and the resulting mixture was reacted in a PFA capillary coil (0.2 mL internal volume, 1 min residence time) at either 0 °C (kinetic conditions) or 25 °C (thermodynamic conditions). The reactor effluent was next mixed through a PEEK T-mixer with 1-chloro-1-nitrosocyclopentane (**1a**, 0.5 M in MTBE, 0.11 mL min⁻¹). The resulting mixture was reacted in a PFA capillary coil (0.31 mL internal volume, 1 min residence time) at 0 °C. The reactor effluent was next mixed through a PEEK T-mixer with an aqueous solution of HCl (6 M) injected with a pump set to 0.3 mL min⁻¹. The mixture was reacted in a PFA capillary coil (0.61 mL internal volume, 1 min residence time) at 60 °C. The entire setup was operated under 5 bar of counterpressure. A final liquid–liquid membrane separator was inserted downstream and the aqueous retentate was collected at steady state, diluted with MeOH, and analyzed by HPLC/DAD (kinetic conditions: **3v-1**, 77% conv., 66% isolated yield; thermodynamic conditions: **3v-2**, 81% conv., 71% isolated yield).

Pilot scale α -aminohydroxylation of enolizable ketones **2b and **2k**.** The pumps used to deliver the enolates derived from

propiophenone **2b** and 1-(3-chlorophenyl)propan-1-one **2k** (0.5 M in dry THF) and **1a** (0.5 M in MTBE) were both set to 30 mL min⁻¹ and injected in a Corning® Advanced-Flow™ G1 SiC Reactor (6 fluidic modules connected in series, 48 mL internal volume, 48 s residence time at 0 °C). The reactor effluent was directly collected in aqueous HCl (1 M) under vigorous stirring to hydrolyze the intermediate nitron (**nit-2b,2k**). Conversion and isolated yield: starting from propiophenone **2b** (**3b**, 98% conv., 82% isolated yield) or 1-(3-chlorophenyl)propan-1-one **2k** (**3k**, 88% conv., 73% isolated yield).

Semi batch preparation of norephedrine. The aqueous reactor effluent from the previous pilot scale experiment with **2b** was poured in a separatory funnel in the presence of 250 mL of HCl (1 M) and extracted with Et₂O (3 × 250 mL). The aqueous layer was concentrated under vacuum and the crude residue was dissolved in 700 mL of MeOH. Subsequently, 40.7 g (1.1 mol, 2.2 equiv.) of NaBH₄ were added portion wise over 60 min and the mixture was stirred for 2 h at 0 °C. Then, 3 M HCl (400 mL) were added to adjust the pH to 1. The solvent (MeOH) was then removed under reduced pressure and 700 mL of a 2:1 HCl/AcOH mixture were added to the resulting solution. Afterwards, 162.5 g (2.5 mol, 5 equiv.) of zinc dust were added at 0 °C and the resulting suspension was vigorously stirred for 3 days at room temperature. The resulting solid residue was removed by filtration and the pH of the filtrate was adjusted to 14 using a 50 wt% sodium hydroxide aqueous solution. Brine (250 mL) was added and the crude reaction mixture was extracted with Et₂O (5 × 500 mL) to give a colorless ethereal solution. The ethereal solution was dried over MgSO₄, filtered and concentrated under reduced pressure to give crude norephedrine as a white solid. The solid was then recrystallized in Et₂O/hexane (1:2) to give 43 g (59% overall isolated yield) of pure norephedrine.

Results and discussion

Continuous flow preparation of α -chloronitroso species

α -Chloronitroso species are typically prepared from a variety of substrates,^{85–89} although the corresponding oximes are typically privileged substrates. The most represented protocols use chlorine-based oxidizers. Procedures based on chlorine gas were amongst the earliest reported.^{65,84,90–96} Given the hazards related with the handling of Cl₂ gas on a preparative scale, a procedure relying on its *in situ* generation from aqueous H₂O₂/HCl was reported by Terent'ev for the preparation of various α -chloronitroso compounds.⁹⁷ Alternative methods based on *N*-chloroderivatives such as *N-tert*-butyl-chlorocyanamide,⁹⁸ *N,N'*-dichloro bis(2,4,6-trichlorophenyl)urea,⁹⁹ 1-chloro-1*H*-benzo[*d*][1,2,3]triazole,⁷⁹ or *N*-chlorosuccinimide,⁸² provided a low atom economy¹⁰⁰ and a high environmental factor (*E*-factor).¹⁰¹ Hypochlorites have attracted attention for converting oximes into α -chloronitroso compounds since the early 1960s,¹⁰² and either inorganic¹⁰³ or organic^{38,102} hypochlorites can be utilized. Among organic hypochlorites, *t*BuOCl (Fig. 4) emerged as a convenient and readily available reagent. The

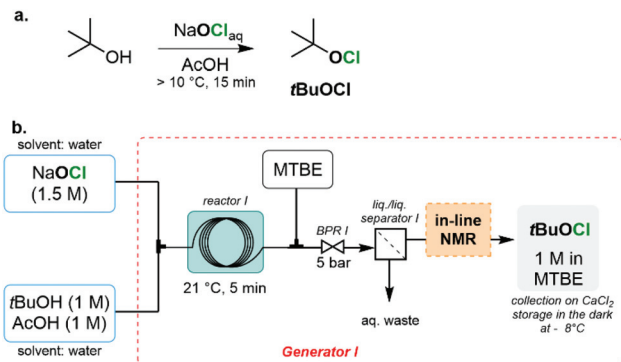


Fig. 4 (a) The method of Mintz and Walling⁸¹ for the preparation of **tBuOCl** in batch. (b) Simplified microfluidic flowchart (Generator I) for the preparation of *tert*-butyl hypochlorite (**tBuOCl**) showcasing the extraction module. The column packed with glass beads upstream the membrane separator is omitted for clarity (ESI for details, section 1.5.1†). An in-line, low field NMR can be inserted downstream to monitor the conversion of **tBuOH** into **tBuOCl** (see ESI section 2.2.3†).

first procedures were reported using trichlorofluoromethane as solvent, a banned chemical responsible for the ozone layer depletion.³⁸

A typical procedure for the preparation of **tBuOCl** follows an adaptation of the method of Mintz and Walling⁸¹ and consists of reacting sodium hypochlorite with *tert*-butanol in the presence of acetic acid at 0 °C in the dark (Fig. 4a). Commercial bleach can advantageously replace aqueous solutions of reagent grade sodium hypochlorite. The formation of **tBuOCl** is almost instantaneous, and it separates from the aqueous reaction mixture. The absence of precipitates makes the transposition under continuous flow conditions straightforward, yet it was never reported.

tBuOCl is an extremely potent electrophilic chlorinating agent that offers one of the most convenient and atom-economic procedures for accessing α -chloronitroso species from oximes. Unlike chlorine, its handling is facilitated by its liquid nature, although its toxicity, photo- and thermal instability raise significant safety concerns even for lab scale operation. Handling of *tert*-butyl hypochlorite as a secondary oxidizer thus justifies a flow protocol to maintain discrete amounts at any time upon operation. The formation of **tBuOCl** is conveniently achieved from widely accessible commercial compounds, including aqueous NaOCl, AcOH and **tBuOH**. Under continuous flow, the formation of **tBuOCl** is completed (>99% conversion) within 5 min of residence time with an optimal NaOCl/**tBuOH**/AcOH ratio of 1.5 : 1 : 1 (Fig. 4b).

Generator I was constructed from PFA coils and HPLC-type connectors. In a typical procedure, a feed solution of NaOCl in water (1.5 M) and a feed solution of **tBuOH** (1 M) and AcOH (1 M) in water were injected at 0.1 mL min⁻¹ through a static T-mixer and reacted for 5 min at 25 °C in a PFA coil; a stream of MTBE was injected downstream to extract **tBuOCl**. Although **tBuOCl** is poorly soluble in aqueous medium, its recovery through membrane separation was drastically enhanced upon

extraction with an organic solvent. Chlorinated solvents such as dichloromethane and chloroform gave high extraction efficiency and facilitated the in-line NMR monitoring of the reaction, yet their environmental impact led us to consider MTBE as a greener alternative. Compared to other ethereal solvents, MTBE is considered as a safer option since it does not form potentially explosive peroxides and does not react with **tBuOCl**.^{65,104} A column packed with glass beads ($\phi = 0.1$ mm) was inserted before the membrane separator to enhance the extraction efficiency, giving **tBuOCl** in 98% yield (ESI, Fig. S1 and Table S3†). The aqueous effluent from the membrane separator was collected in a waste. The ability to produce **tBuOCl** in a first generator and to directly use it downstream for reaction with oximes enhances process safety, since it avoids its isolation and storage. Adjustment of the flow of MTBE enabled the preparation of a 1 M solution. During the preliminary development stages of the flow process toward **tBuOCl**, off-line redox titration was carried out to determine its concentration after extraction (ESI, section 2.2.2†). After optimization, off-line titration was conveniently replaced with in-line low field ¹H NMR monitoring (ESI, section 2.2.3†). The organic effluent can be collected over CaCl₂ and stored at low temperatures, preferably in a brown glass bottle. Samples could be maintained accordingly for several months, yet a direct concatenation to downstream operations is highly desirable for mitigating chemical hazards.

Since the cyclopentyl and cyclohexyl nitroso derivatives **1a,b** are the most described α -chloronitroso reagents for electrophilic amination reactions in the literature,^{57–62,65} they were selected as model compounds for the optimization of Generator II (Fig. 5b). The corresponding cyclopentanone and cyclohexanone oximes **4a,b**, respectively, are readily available

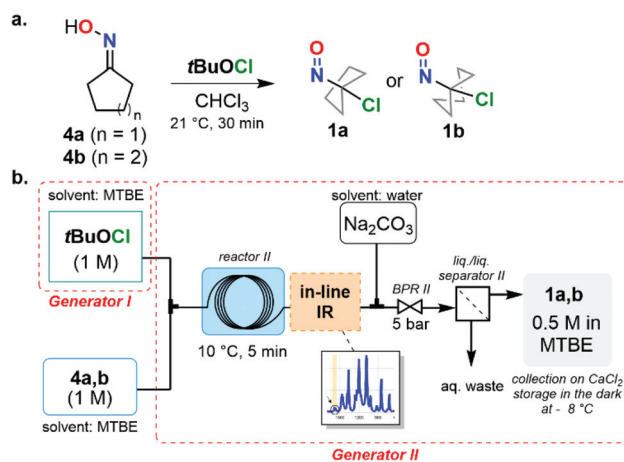


Fig. 5 (a) Use of **tBuOCl** for the conversion of oximes **4a,b** into the corresponding α -chloronitroso species **1a,b**. The advancement of the reaction can be qualitatively monitored with the appearance of the typical blue color of nitroso derivatives **1a,b**. Typical reaction conditions imply the slow addition of **tBuOCl** at room temperature over 30 min. (b) Simplified microfluidic flowchart for Generator II for the production of model α -chloronitroso species **1a,b** showcasing the in-line IR and the extraction module.

and can be ordered on the multikilogram scale (Fig. 5a). The next step thus consisted in the downstream use of *t*BuOCl for the conversion of oximes **4a,b** into **1a,b** (Fig. 5b).

One of the main challenges for optimizing the second generator relied on the appropriate selection of an off- or in-line analytic protocol to monitor reaction optimization. The unstable nature of α -chloronitroso species precluded direct isolation and characterization *via* typical off-line analytic procedures such as NMR, GC and HPLC. We opted for non-destructive in-line IR spectroscopy (ESI, section 2.2.18[†]), providing a very convenient protocol to optimize reaction parameters by monitoring the relative variations of the specific vibration bands of the starting oxime ($\tilde{\nu}_{OH} = 3550\text{--}3600\text{ cm}^{-1}$, $\tilde{\nu}_{CN} = 1665\text{--}1720\text{ cm}^{-1}$) and of the corresponding nitroso derivatives ($\tilde{\nu}_{NO} = 1539\text{--}1621\text{ cm}^{-1}$).

The organic effluent coming from the upstream Generator I, consisting of a 1 M solution of *t*BuOCl in MTBE, was then redirected to the upstream section of the Generator II (Fig. 5b), where it was mixed with a solution of oxime **4a** (1 M in MTBE, 0.1 mL min⁻¹) and reacted at 10 °C for 5 min in a PFA coil. The reactor effluent was continuously extracted with an aqueous 10 wt% Na₂CO₃ solution and separated through hydrophobic membrane technology. The final extraction was paramount to remove traces of acetic acid, *t*BuOH and other by-products that would otherwise interfere with downstream operations. The aqueous stream was redirected to a waste and the organic permeate was collected. Residual water in the organic stream (**1a** in MTBE) was determined by Karl-Fisher titration (ESI, section 2.2.19[†]). The titration results emphasized that the membrane performed very well, with a residual water content of 19 ppm in the organic MTBE permeate; further drying with MS 3 Å decreased the moisture content to 3 ppm. Downstream telescoping with the actual α -aminohydroxylation would therefore require the addition of a drying column filled with MS 3 Å on the permeate prior to injection over enolates (see section “ α -Aminohydroxylation on model ketones **2a,b**” below).

The conversion toward compound **1a** was quantitative, and the process was extended for the production of **1b** and performed likewise. The organic effluent can be collected over CaCl₂ and stored at -8 °C, preferably in a brown glass bottle. Samples could be maintained accordingly up to 2 weeks, yet a direct concatenation to downstream operations is highly desirable. In view of the preparation of *rac*- α -aminohydroxylated ketones, the development of a reliable Generator II of nitroso **1a,b** was considered as sufficient milestone, although Generator II was also amenable for the preparation of a small library of other α -chloronitroso derivatives (see ESI section 2.2.17[†] for details) upon minor temperature adjustments.

Assessment of scalability for Generators I–II

With the optimization of Generators I–II on the microfluidic scale, we next envisioned its progressive scalability from lab to pilot scales. The first step of the transposition relied on a modular Corning® Advanced-Flow™ Low Flow reactor. The mesofluidic setup consisted of glass fluidic modules (0.5 mL

each) embedded with a heat exchanger and connected in series to mimic the microfluidic configuration of Generators I–II (Fig. 4b and 5b). Upon minimal readjustment of the process conditions (ESI, section 2.2.13[†]), the process was then transposed to pilot scale with a modular Corning® Advanced-Flow™ G1 reactor (Fig. 6).

The transposition of Generator I to the pilot scale involved 2 G1 fluidic modules (FMs) connected in series (8 mL internal volume each) and operated at 25 °C for the reaction of an aqueous solution containing *tert*-butanol (1 M) and acetic acid (1 M) with aqueous sodium hypochlorite (2.25 M) within 36 s of residence time. The effluent from Generator I was mixed with a stream of MTBE and the extraction of *t*BuOCl was performed in an additional FM (8 mL internal volume) operated at 25 °C. The resulting biphasic stream was next processed through a pilot scale membrane separator (Zaiput Flow Technologies liquid–liquid separator SEP-200) equipped with a PTFE hydrophobic membrane (1 μ m pore size). Qualitative monitoring was carried out through in-line low field ¹H NMR (ESI, section 2.2.3[†]). The MTBE permeate (*t*BuOCl, 1 M) was next redirected to Generator II, where it quantitatively reacted with oximes **4a,b** into another FM (8 mL internal volume) operated at 10 °C with a residence time of 18 s (Fig. 6).

The outlet of Generator II was connected through a sampling loop to an in-line IR spectrometer for real-time monitoring. The reactor effluent was collected in a tank containing a solution of triphenylphosphine (1 M) for chemical destruction.^{84,105,106} Once the generation of nitroso was validated on the pilot scale, the α -aminohydroxylation step was considered.

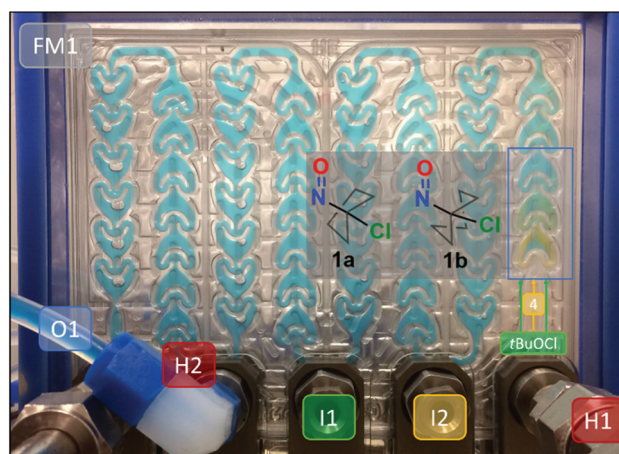


Fig. 6 Close-up of the pilot scale Generator II relying on an 8 mL internal volume Corning® Advanced-Flow™ G1 reactor fluidic module with integrated HEART™-shape static mixers (courtesy of Corning®). The total residence time is 18 s, yet the characteristic blue color accompanying the formation of α -chloronitroso **1a,b** appears nearly instantaneously after the injection of *t*BuOCl and oximes **4a,b**. FM1: fluidic module; H1,2: in/outlets for thermofluid; I1: inlet for *t*BuOCl (1 M MTBE, feeding from backside); I2: inlet for oximes **4a,b** (1 M MTBE, feeding from backside); O1: outlet for α -chloronitroso **1a,b** in MTBE.

α -Aminohydroxylation on model ketones 2a,b

The ability to produce a reliable and steady stream of **1a,b** opens up new possibilities for downstream electrophilic amination setup. We shifted gears for revisiting Oppolzer's^{57–62} electrophilic amination under continuous flow conditions. Two simple enolizable ketones were selected as model substrates: acetophenone **2a** and propiophenone **2b**. While the electrophilic amination with ketone **2a** was never reported in the literature, **2b** served as a privileged target in Oppolzer's work, since it is a fast track entry toward (pseudo)ephedrine and related APIs. **2b** would hence set boundaries and would help us to calibrate our protocol.

The typical procedure in Oppolzer's original papers relied on the formation of a sodium enolate at low temperature, followed by the electrophilic amination with **2b** in the presence of a Lewis acid, such as ZnCl_2 or $\text{Zn}(\text{OTf})_2$. A direct transposition under microfluidic conditions systematically led to clogging. However, computations on model compounds indicated that the reaction in the presence and in the absence of ZnCl_2 provides similar reaction profiles, hence indicating that Zn^{2+} catalysis is in fact not mandatory for this reaction (ESI, sections 2.2.7 and 4.1†). Accordingly, going back to batch preliminary optimizations (Fig. 7), lithium bis(trimethylsilyl)-amide (LiHMDS) was identified as the best performing base for the rapid and complete enolization of **2b** in the presence of nitroso compounds **1a,b** (ESI, section 2.2.14†) and in the absence of any Lewis acid at -78°C in THF/MTBE (30 min

total reaction time). LC monitoring however indicated that the reaction with cyclopentyl α -chloronitroso **1a** was faster and more selective than with **1b**. This observation was further confirmed under microfluidic conditions (ESI, section 2.2.16†), hence further trials were only conducted with **1a**.

Complete conversion to nitrone **nit-2b** was reached after 90 min in batch. Nitrone **nit-2b** was next hydrolyzed with aqueous HCl (1 M) for 12 h at room temperature, leading to the desired α -aminohydroxylated ketone *rac*-**3b** (in 90% isolated yield; Fig. 7a). From this preliminary optimization, it came out that the slow addition of **1a** at low temperature was critical to avoid vigorous exothermic decomposition. With this in hand, the α -aminohydroxylation was attempted on acetophenone **2a**. The conversion was complete, yet the product obtained was not the expected α -aminohydroxylated ketone **3a**, but amidoxime **5** (Fig. 7a), the structure of which was confirmed by X-ray diffraction.¹⁰⁷ We reasoned that the formation of **5** would occur from two consecutive α -aminohydroxylations on **2a**. Further optimizations did not yield the desired α -aminohydroxylated ketone compound (**3a**).

In order to identify the main parameters governing the reactivity and the selectivity of the α -aminohydroxylation, computations (see ESI, section 4.2†) were undertaken starting from the lithium enolates **en-2a** and **en-2b** (Fig. 7b). Experimentally, a second amination is only observed in the case of **2a**, leading after hydrolysis to amidoxime **5**. Our calculations predicted that for both **en-2a** and **en-2b**, the electrophilic amination with **1a** proceeds with no enthalpy barrier, meaning that it is extremely fast and diffusion-controlled. The main hypothesis was that the second electrophilic amination proceeds through deprotonation of **nit-2a,b** by enolate **en-2a,b** to form **en-nit-2a** and **en-nit-2b**, respectively. The latter would then add onto another equivalent of **1a** to yield bisnitrono adducts (**bis-nit-2a** and **bis-nit-2b**) upon the elimination of chloride. These latter would next undergo acidic hydrolysis to yield the corresponding amidoximes, yet experimentally this only happens for **2a**. Our computational study revealed that the acid–base equilibrium toward **en-nit-2a** and **en-nit-2b** involves a low free energy barrier ($\Delta G^\ddagger = 3.7$ and 9.4 kcal mol⁻¹ for **nit-2a** and **nit-2b**, respectively) and is highly displaced toward the formation of **en-nit-2a** and **en-nit-2b** ($\Delta G = -22.8$ and -19.7 kcal mol⁻¹ for **en-nit-2a** and **en-nit-2b**, respectively). Subsequent addition onto cyclopentyl α -chloronitroso **1a** occurs with a free energy barrier of 11.4 and 19.5 kcal mol⁻¹ for **en-nit-2a** and **en-nit-2b**, respectively. These results indicate that the selectivity for the first amination vs. the second amination must be determined by the competition between the addition onto **1a** and the deprotonation of **nit-2a** and **nit-2b**, respectively. In both cases, for **en-2a,b**, the addition onto **1a** (first amination) is diffusion-controlled (*vide supra*). Concerning the deprotonation, for **nit-2a**, it involves a free energy barrier of 3.7 kcal mol⁻¹, meaning that the rate of this step ($k \sim 6.10^9$ M⁻¹ s⁻¹) is also at, or very close to, the diffusion limit. In the case of **nit-2a**, the free energy barrier is higher (9.4 kcal mol⁻¹), predicting a rate significantly lower than the diffusion limit ($k \sim 2.10^5$ M⁻¹ s⁻¹).

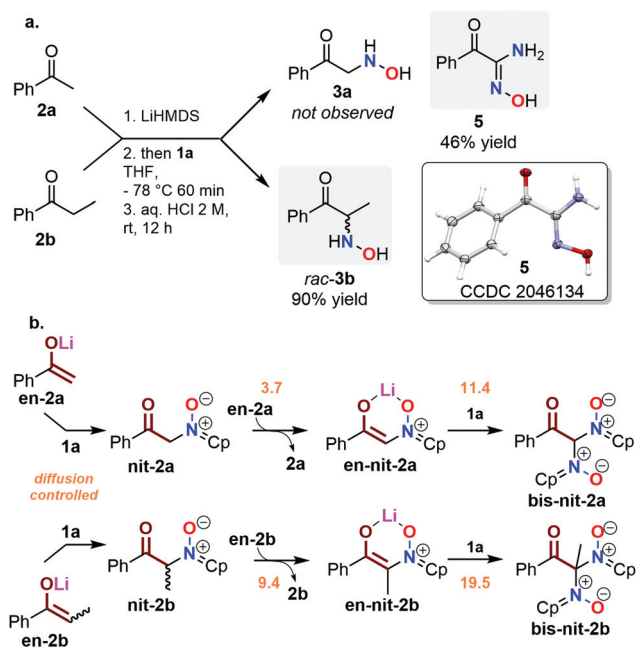


Fig. 7 (a) Electrophilic amination of acetophenone **2a** and propiophenone **2b** with cyclopentyl α -chloronitroso **1a** under optimized conditions. (b) Computations at the B3LYP-D3/6-311+G**(MTBE)//B3LYP-D3/6-31+G*(MTBE) level of theory for the electrophilic amination of the enolates of acetophenone (**en-2a**) and of propiophenone (**en-2b**), respectively. Free energy barriers are indicated in orange (kcal mol⁻¹). Cp = cyclopentyl. See ESI (section 4.2†) for details.

From our computational study, it became clear that in the case of ketone **2a**, the second amination is competitive, hence leading to the bis-amination product **5** in the presence of a local excess of enolate **en-2a**. Any inhomogeneity in the reaction mixture (typically related to inefficient mixing in batch) leads to poor control of the local stoichiometry, hence triggering side reactions. It is now well accepted that reactions sensitive to local stoichiometry can be advantageously developed under continuous flow conditions, often with a significant reduction in side reactions.^{74,108}

With this mechanistic understanding, we envisioned the transposition of the electrophilic amination of model ketones **2a,b** under microfluidic conditions. Three steps had to be implemented according to a concatenated microfluidic setup relying on three modules (Fig. 8a). The first module was dedicated to the enolization of ketones **2a,b** with LiHMDS. The improved heat exchange efficiency under continuous flow conditions is typically exploited to perform highly exothermic reactions at higher temperatures than batch would normally allow.^{108,109} Upon optimization, the enolization of ketone **2a** in module I required 1 min of residence at 0 °C with 1.1 equiv. of LiHMDS in THF (0.5 M), rather than typically -78 °C in batch. The effluent of module I was then directly mixed with a stream of **1a** (0.5 M in MTBE), in provenance from Generator II that was operated continuously to feed the electrophilic amination.

Screening of the electrophilic amination conditions on model ketones **2a,b** emphasized that the electrophilic amination reaction could advantageously be performed at a much higher temperature in flow (0 °C) than in batch (typically -78 °C), while avoiding decomposition and reaching almost quantitative conversion within 1 min of residence time (Fig. 8b). Higher temperatures than 0 °C for shortening the residence time even further are not advised in flow since two runs at room temperature led to the explosive decomposition of the reaction mixture.

The final hydrolysis of nitrone **nit-2a,b** was performed in module III. The effluent from module II was immediately mixed with aqueous HCl (6 M) at 0.3 mL min⁻¹ and reacted in a PFA coil. Increasing the temperature from room temperature to 60 °C in module III led to a significant reduction in reaction time, conversions up to 97% being attained within 1 min. The conversion of ketones **2a,b** was of 70 and 96%, respectively, with a quantitative selectivity within 3 min of total residence time toward the desired α -aminohydroxylated ketones **3a,b** (as their hydrochlorides), with no traces of the bisamination product **5**. The fast mixing and fine control on the local stoichiometry, as well as the effective concatenation helped suppressing the occurrence of an amidoxime by-product **5**. Besides, the electrophilic amination on primary enolizable ketones was never reported with nitroso derivatives.

A final in-line membrane separation step was integrated to module III to effect continuous separation between the aqueous stream containing essentially pure **3a,b** as their hydrochlorides and the organic effluent containing traces of unreacted nitroso **1a** and any other organic by-products (ESI, section 2.2.20†). The design of the downstream extraction was

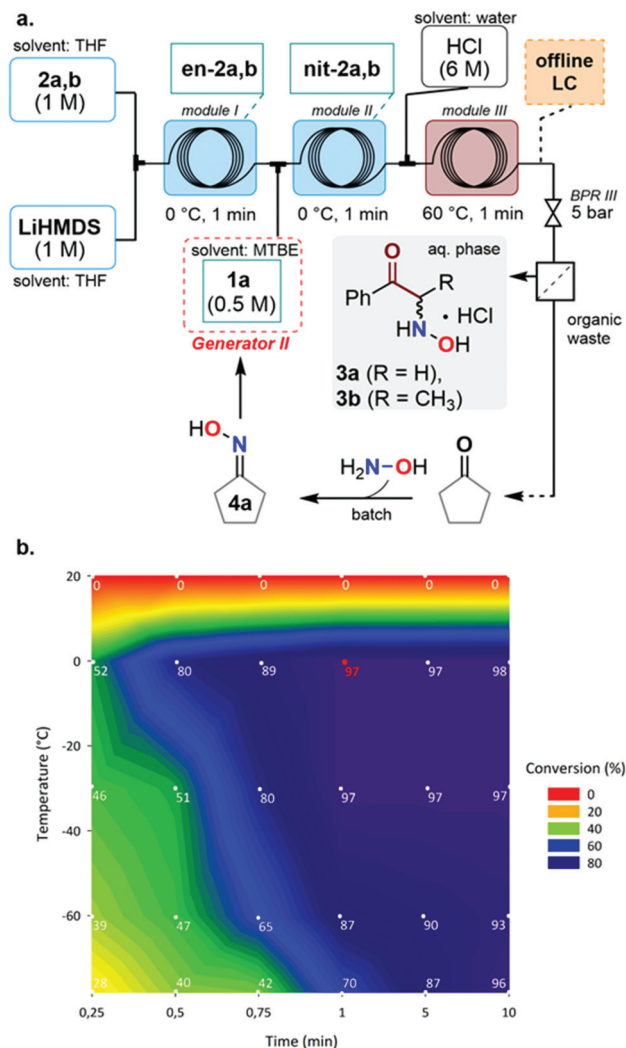


Fig. 8 (a) Fully concatenated setup showing Modules I (enolization), II (electrophilic amination, connected upstream to Generator II) and III (hydrolysis) for the electrophilic amination of enolizable ketones **2a,b** with α -chloronitroso **1a**. The organic permeate was further processed to recover cyclopentanone, which could be converted back to cyclopentanone oxime **4a** with 83% yield and could be used to feed Generator II. (b) Screening of the reaction conditions for the electrophilic amination of model substrate **2b** with nitroso **1a** under continuous flow conditions. The number in the isovalue plot indicates the HPLC conversion of **2b**. At room temperature, exothermic decomposition of nitroso **1a** occurred leading to either clogging or rupture of module II.

carefully engineered in order to avoid the contamination of active pharmaceutical ingredient intermediates with potentially toxic nitroso compounds.

The insertion of a hydrophobic membrane separator, combined with an upstream hydrolysis with hydrochloric acid, provided a simple yet elegant and robust solution to segregate the nitroso-containing organic permeate from the α -aminohydroxylated ketone hydrochlorides in water. The organic permeate was treated with PPh₃ (1 M in THF) to neutralize any leftover of **1a**. The aqueous effluent was collected, and processed to recover **3a,b** as free bases (ESI, section 2.2.7†). The

aspects of recovering and reusing the nitroso carbon backbone from the organic permeate were also considered. The permeate was further processed to recover cyclopentanone, that could be converted back to cyclopentanone oxime **4a** with 83% isolated yield (ESI, section 2.2.9†). The recovery of the carbon backbone of nitroso **1a** significantly reduces the overall footprint of the process, since the cyclopentyl backbone is only borrowed as a vehicle for transferring a hydroxylamine electrophilic synthon to the enolizable ketone substrate (Fig. 8a).

Scope of the α -aminohydroxylation with nitroso **1a**

With a fully functional continuous flow system including a chemical generator for nitroso species **1a** and a modular setup for the electrophilic amination of model enolizable ketones, we aimed at pushing further the horizon of the microfluidic setup. An ideal scenario would be to keep the same setup while only changing the feed solution of enolizable ketone substrates and assess its potential for the edition of discrete libraries of α -aminohydroxylated ketones. Following this idea, the setup was left unchanged and the reactor was fed with various enolizable ketones (Fig. 9 and 10), preferably bearing an aromatic ring to facilitate off-line LC monitoring.

We began exploring the scope of this protocol with derivatives of propiophenone **2b-l**, from which several biologically active molecules can be accessed through this procedure, including norephedrine (from **3b**), cathinone (from **3b**), mephedrone (from **3c**) and bupropion (from **3k**).

Feed solutions of ketones **2b-l** were prepared in dry THF (0.5 M) and successively subjected to electrophilic amination with nitroso **1a**, giving the corresponding hydrochlorides of α -aminohydroxylated ketones *rac*-**3b-l**. Neutralization, followed by extraction in MTBE and evaporation gave *rac*-**3b-l** free bases in 49–95% isolated yield (for some examples, the hydrochloride was isolated and analyzed, see ESI, sections 2.3, 2.5 and 2.6†). Analytical samples were obtained through either recrystallization or after column chromatography on silica gel. The lowest conversion and isolated yield concerned *rac*-**3l** that features an *ortho*-CF₃ group, which might sterically hamper the reaction. For all other propiophenone-related substrates, EWG-substituted derivatives came with a slightly lower conversion, which most likely relates to a lower nucleophilicity of the corresponding enolates. The difference with EDG-substituted propiophenone derivatives is, however, difficult to exploit according to a Hammett relationship.

The conditions are also amenable to heteroaromatic ketone **2m** (93% conv.) and sterically more demanding **2n** (83% conv.) and **2o** (76% conv.). Besides secondary ketones (**2b-p**), the electrophilic amination under flow conditions was also successfully applied to a variety of tertiary enolizable ketones, hence providing quaternary α -aminohydroxylated ketones **3q-u** in good to high isolated yields (72–84%). Unexpected oxidation products were obtained for two additional substrates (diethyl malonate and 2-phenylacetophenone) that are only described in the ESI (sections 2.3, 2.5 and 2.6†).

Our interest toward ketamine and analogs⁷⁵ prompted us to consider (*rac*)-2-phenylcyclohexanone (**2v**) as a substrate. In

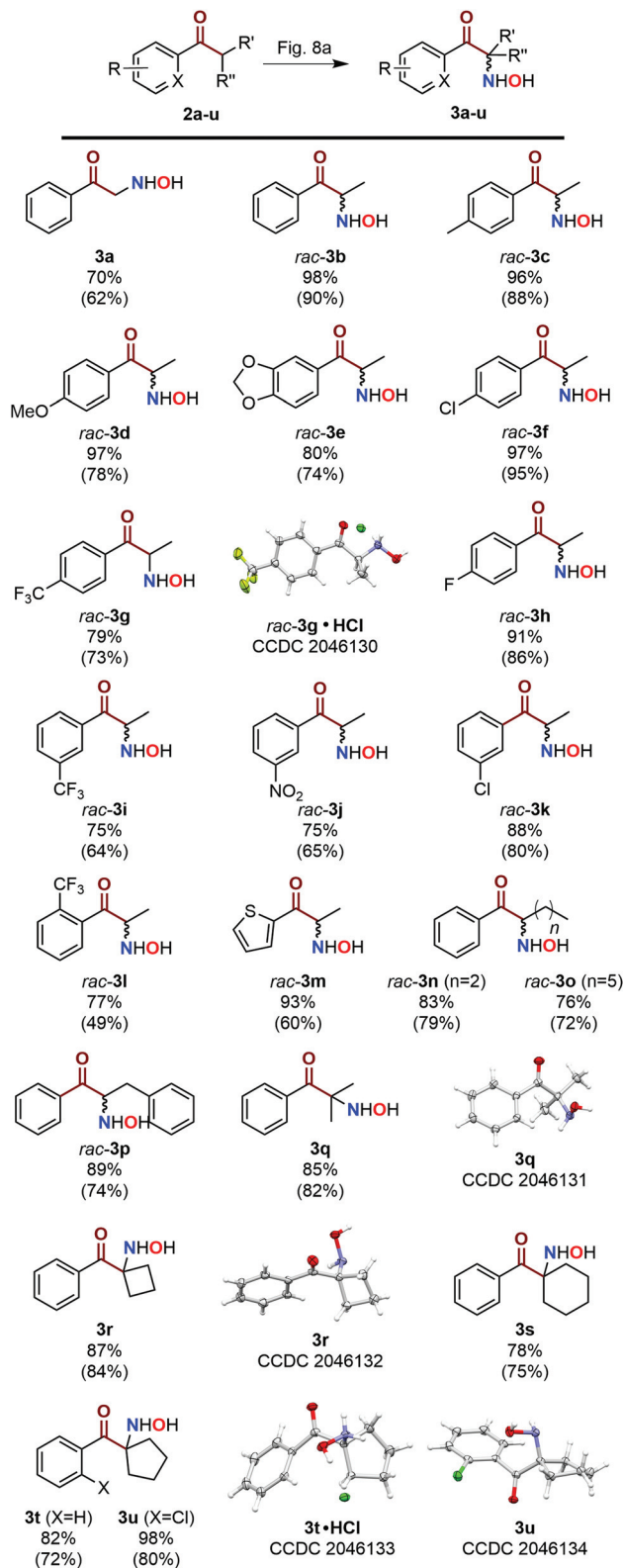


Fig. 9 Scope of the electrophilic amination on primary, secondary and tertiary ketones. Conversion and isolated yield (in parentheses) are indicated. All compounds were obtained according to the setup described in Fig. 8a. See also Fig. 10.

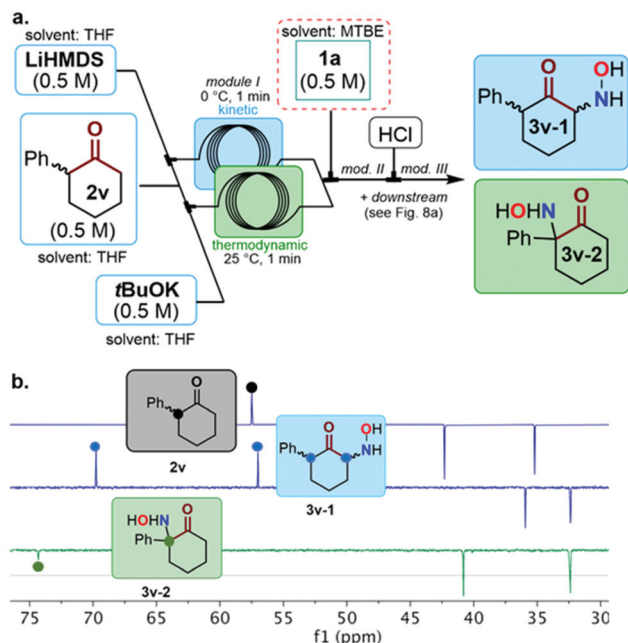


Fig. 10 (a) Adaptation of the microfluidic setup to 2-phenylcyclohexanone (**2v**) for the electrophilic amination under kinetic or thermodynamic conditions. (b) Details of the area of interest for the ^{13}C APT spectra of the kinetic and thermodynamic α -aminohydroxylated ketones **3v-1,2** compared to the starting ketone **2v**.

contrast to the other substrates of the study, **2v** bears two potentially enolizable positions, hence providing either a direct precursor of norketamine and ketamine (**3v-2**) or an analog (**3v-1**, Fig. 10). The selectivity between the two enolizable sites is a classical control of kinetic vs. thermodynamic conditions for the generation of the corresponding enolates *kin-en-2v* and *therm-en-2v*. Module I of the microfluidic platform described in Fig. 8a was adapted accordingly (Fig. 10): the formation of *kin-en-2v* was obtained as previously, within 1 min of residence time at 0 °C with LiHMDS (0.5 M in THF), while the formation of *therm-en-2v* was performed at room temperature, within 1 min of residence time with *t*BuOK (0.5 M in THF). The rest of the setup was left unchanged.

Under kinetic conditions for the formation of the enolate, the electrophilic amination occurred selectively at the least substituted position, thus leading to the formation of the corresponding secondary α -aminohydroxylated ketone **3v-1** in 66% isolated yield (77% conv.). With module I operated at room temperature for the enolization of **2v** with *t*BuOK, the electrophilic amination occurred selectively at the thermodynamic position, yielding α -aminohydroxylated ketone **3v-2** in 71% isolated yield (81% conv.).

Assessment of scalability for the electrophilic amination

With a wide chemical compatibility and the potential for rapidly accessing libraries of structurally diverse α -aminohydroxylated ketones, this method has proven its added-value for R&D applications. In the next stage of the project, we wanted to assess the scalability of the critical electrophilic amination step. The setup

was simplified to spare resources, and we focused the efforts on the most critical steps (module 2). The hydrolysis of the nitron was carried out in a collection tank. Two pharmaceutically relevant intermediates were selected as demonstrators, namely, 2-(hydroxyamino)-1-phenylpropan-1-one (*rac-3b*) and 1-(3-chlorophenyl)-2-(hydroxyamino)propan-1-one (*rac-3k*), which are advanced intermediates for the preparation of norephedrine and bupropion, respectively.

The process was then transposed to pilot scale with a Corning® Advanced-Flow™ G1 SiC Reactor (ESI sections 1.5.8 and 2.2.21†). Silicon carbide was selected here rather than glass to avoid any corrosion issue with LiHMDS. The setup for the pilot scale α -aminohydroxylation involved several G1 SiC FMs connected in series (about 48 mL total internal volume) and operated at 0 °C. To simplify the setup, preformed solutions of the enolates (0.5 M) derived from **2b** (*en-2b*) or **2k** (*en-2k*) were prepared by mixing LiHMDS with the enolizable substrate and maintaining the feed solutions at 0 °C. The reactor effluent from pilot scale Generator II was dried with MS 3 Å and was reacted with enolates *en-2b,k*. With a total flow rate of 60 mL min⁻¹, a shorter residence time than for the microfluidic scale was obtained (48 s). The reactor effluent was collected directly in aqueous HCl (1 M) to perform the hydrolysis of the intermediate nitrones *nit-2b,k* toward the corresponding α -aminohydroxylated ketones *rac-3b* and *rac-3k* in the collection flask. Samples were collected at steady state and hydrolyzed prior to LC analysis. Daily productivities of 3.49 kg (98% conv., 82% isolated yield) and of 3.19 kg (88% conv., 73% isolated yield) were achieved for *rac-3b* and *rac-3k*, respectively. Both compounds were further reduced in batch for the preparation of norephedrine and analogs.

Discussion on the overall footprint of the electrophilic amination

Besides the unquestionable safety assets of such an integrated platform that concatenates two upstream continuous flow generators of highly reactive species (*t*BuOCl and nitroso **1a**), its versatility was also demonstrated through the generation of libraries of structurally diverse α -aminohydroxylated ketones. On the microfluidic scale, the electrophilic amination platform could be deployed for feeding upstream the process of discovery of new hits/leads in medicinal chemistry, or at least accelerating the preparation of α -aminoketone and β -amino alcohol scaffolds. Besides operation at the lab scale, we have also demonstrated the scalability of each step, opening up perspectives on the production scale with low footprint reactors. The fully concatenated system, including Generators I–II and the 3 modules for the electrophilic amination step was successfully transposed to pilot scale in a commercial mesofluidic reactor with a minimal footprint ($L \times W \times H$ 94 × 42 × 40 cm), excluding the auxiliaries, *i.e.* pumps, thermostats and in/off-line analytical devices. The assets of flow chemistry were clearly demonstrated in terms of high heat exchange efficiency (with reactions performed at much higher temperatures than conventional batch processes) and in terms of mixing efficiency and control over the local stoichiometry (with the suppression of a bisamination by-product for a model primary ketone).

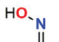
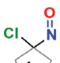
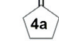

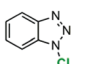
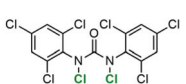
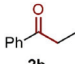
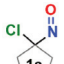
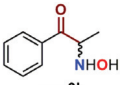
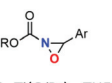
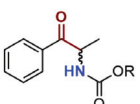
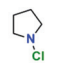
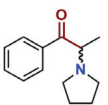
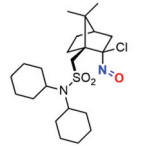

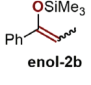
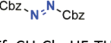
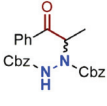
Besides process performance, the chemistry developed is also advantageous according to its calculated environmental factor (*E*-factor) (ESI, section 3.1†). The *E*-factor was calculated according to the equation [*E*-Factor = (mass of total inputs) – (mass of valuable products)/mass of valuable products] and following the recommendations of Andraos.¹¹⁰ The two main elements of the process, namely the preparation of nitroso **1a** and the electrophilic amination on acetophenone **2b** as a model substrate, were compared with similar strategies reported in the literature, and their respective *E*-factors were calculated and compared (see Table 1). As a brief reminder, *E*-factor values inherently relate to the nature of the process

(<0.1 for oil refining; <1–5 for bulk chemicals; 5–50 for fine chemicals and 25–100 for pharmaceuticals). Since the context of this research is at the interface between fine chemicals and pharmaceuticals, an *E*-factor comprised between 5–100 would be acceptable.

From the analysis of the *E*-factors presented in Table 1, it can be seen that our electrophilic amination procedure is very favorable (entry 1). It outclasses previous protocols for the preparation of nitroso **1a** with an *E*-factor = 6. It is also worth mentioning that the carbon backbone of **1a** is recyclable (see above). For the electrophilic amination, one can see from Table 1 that a calculated *E*-factor of 11 was obtained for this protocol (entry 5), which is very competitive given the complexity of the sequence, despite the fact that the protocol produces racemic α -aminohydroxylated ketones (enantioselective version: see entry 8, *E*-factor = 26).

A more refined analysis was next performed using the semi-quantitative EcoScale from EcoSynth.^{114,115} The EcoScale considers various parameters with a direct impact on the output of a reaction (*i.e.* yield, costs of chemicals, safety, technical setup, energy requirements, as well as work up & purification). Generator I is associated with an honourable score of 81% on the EcoScale, while Generator II is associated with a score of 76% (ESI, section 3.2†). The electrophilic amination on **2b** as described in this manuscript came with a score of 60% (the calculation does not consider the recycling of the carbon backbone of nitroso **1a** that ultimately makes the process even more appealing), which constitutes a significant improvement compared to the score of 43% obtained for the adaptation of Oppolzer's original amination in batch.

Table 1 Calculated environmental factors (*E*-factors) for the preparation of **1a** and the subsequent electrophilic amination step

Entry	Starting material	Reagents and solvents	Product	<i>E</i> -factor
Preparation of α-chloronitroso 1a				
1		<i>t</i> BuOCl MTBE		6 ^a
2		34% aq. HCl 37% aq. H ₂ O ₂ CH ₂ Cl ₂		32 (ref. 97)
3		 CH ₂ Cl ₂		11 (ref. 79)
4		 CH ₃ CN		12 (ref. 99)
Electrophilic amination on propiophenone 2b and derivatives				
5		 LiHMDS, THF, MTBE		11 ^a
6		 LDA, Ti(O <i>i</i> Pr) ₄ , THF		18 (ref. 111)
7		 L-Proline, Et ₃ N		10 (ref. 112)
8		 NaHMDS, ZnCl ₂ , THF, Et ₂ O		26 (ref. 59)
9		 AgOTf; CH ₂ Cl ₂ , HF-THF		34 (ref. 113)

^aThis work.

Conclusion

This work discloses a unique, scalable and efficient continuous flow strategy for the preparation of libraries of α -aminohydroxylated ketones in good to high isolated yields from the corresponding enolizable ketones and reactive α -chloronitroso **1a**. A library of 22 α -aminohydroxylated ketones was prepared starting from primary, secondary and tertiary ketones, hence opening the way to several intermediates for pharmaceutical production (including WHO essentials and drugs on shortage). The development of a fully concatenated setup, featuring two upstream generators, enables to exploit the unique reactivity profile of α -chloronitroso derivatives to its fullest potential while mitigating chemical risk. The main assets of continuous flow processing, including high heat exchange and mixing efficiencies, the production of discrete amounts of toxic and potentially explosive compounds as well as the integration of in-line analytics were very supportive for the design of a modular, safe and efficient integrated flow protocol. The careful selection of reaction conditions and chemicals, as well as the design of simple yet robust downstream purification and recycling protocols contributed to a significant reduction in overall footprint. Beyond the development of robust conditions in conjunction

with favorable metrics, this work also discloses a versatile platform amenable to either discovery on lab scale or to production at commercial scale. While maintaining a compact and highly integrated reactor setup design (<2 m² including the auxiliaries) for the final demonstrator, a productivity of up to 3.49 kg per day of high value-added α -aminohydroxylated ketone intermediates was achieved. Work is now undergoing for the development of recyclable chiral α -chloronitroso derivatives, which would not only serve as vehicles for NH₂OH, but also for transferring stereochemical information to the ketone substrates.

Conflicts of interest

There are no conflicts to declare.

Acknowledgements

This work was supported by the University of Liège (Welcome Grant WG-13/03, JCMM) and by the F.R.S.-FNRS (Incentive grant for scientific research MIS F453020F, JCMM). Computational resources were provided by the “Consortium des Équipements de Calcul Intensif” (CÉCI), funded by the “Fonds de la Recherche Scientifique de Belgique” (F.R.S.-FNRS) under Grant No. 2.5020.11 and by the Walloon Region. VEK and TT are FRIA PhD fellows. KVH thanks the Research Foundation – Flanders (FWO) (projects AUGÉ/11/029 and G099319N) for funding. RR is a Maître de recherche of the F.R.S.-FNRS. The authors thank Florence Houdouin and Geoffrey Vandendeyck for their experimental support. Dr Guillaume Gauron and Alessandra Vizza (Corning SAS) are acknowledged for the loan of the AFR reactors and the logistic, technical and scientific support for the scalability trials.

Notes and references

- 1 S. Mirabella, F. Cardona and A. Goti, *Org. Biomol. Chem.*, 2016, **14**, 5186–5204.
- 2 M. Grom, G. Stavber, P. Drnovšek and B. Likozar, *Chem. Eng. J.*, 2016, **283**, 703–716.
- 3 B. Robnik, B. Likozar, B. Wang, T. S. Ljubin and Z. Časar, *Pharmaceutics*, 2019, **11**, 1–21.
- 4 M. Trampuž, G. Stavber and B. Likozar, *Chem. Eng. J.*, 2019, **374**, 924–936.
- 5 T. Nobuta, G. Xiao, D. Ghislieri, K. Gilmore and P. H. Seeberger, *Chem. Commun.*, 2015, **51**, 15133–15136.
- 6 Y. Park, Y. Kim and S. Chang, *Chem. Rev.*, 2017, **117**, 9247–9301.
- 7 R. Morodo, R. Gérardy, G. Petit and J.-C. M. Monbaliu, *Green Chem.*, 2019, **21**, 4422–4433.
- 8 A. de la Torre, V. Tona and N. Maulide, *Angew. Chem., Int. Ed.*, 2017, **56**, 12416–12423.
- 9 O. I. Afanasyev, E. Kuchuk, D. L. Usanov and D. Chusov, *Chem. Rev.*, 2019, **119**, 11857–11911.
- 10 R. Dorel, C. P. Grugel and A. M. Haydl, *Angew. Chem., Int. Ed.*, 2019, **58**, 17118–17129.
- 11 Y. Park, Y. Kim and S. Chang, *Chem. Rev.*, 2017, **117**, 9247–9301.
- 12 C. Greck, B. Drouillat and C. Thomassigny, *Eur. J. Org. Chem.*, 2004, 1377–1385.
- 13 A. M. R. Smith and K. K. Hii, *Chem. Rev.*, 2011, **111**, 1637–1656.
- 14 X. Yan, X. Yang and C. Xi, *Catal. Sci. Technol.*, 2014, **4**, 4169–4177.
- 15 K. S. Williamson, D. J. Michaelis and T. P. Yoon, *Chem. Rev.*, 2014, **114**, 8016–8036.
- 16 M. Corpet and C. Gosmini, *Synthesis*, 2014, **46**, 2258–2271.
- 17 T. J. Barker and E. R. Jarvo, *Synthesis*, 2011, **24**, 3954–3964.
- 18 X. Dong, Q. Liu, Y. Dong and H. Liu, *Chem. – Eur. J.*, 2017, **23**, 2481–2511.
- 19 Z. Zhou and L. Kürti, *Synlett*, 2019, **30**, 1525–1535.
- 20 WHO Model Lists of Essential Medicines, <https://www.who.int/medicines/publications/essentialmedicines/en/>, (Accessed on December 28, 2020).
- 21 Drug shortages, <https://www.fda.gov/drugs/drug-safety-and-availability/drug-shortages>, (Accessed on December 28, 2020).
- 22 Shortages catalogue, <https://www.ema.europa.eu/en/human-regulatory/post-authorisation/availability-medicines/shortages-catalogue>, (Accessed on December 21, 2020).
- 23 X. Yang and F. D. Toste, *J. Am. Chem. Soc.*, 2015, **137**, 3205–3208.
- 24 G. A. Shevchenko, G. Pupo and B. List, *Synlett*, 2015, **26**, 1413–1416.
- 25 H. M. Nelson, J. S. Patel, H. P. Shunatona and F. D. Toste, *Chem. Sci.*, 2015, **6**, 170–173.
- 26 X. Fu, H. Y. Bai, G. D. Zhu, Y. Huang and S. Y. Zhang, *Org. Lett.*, 2018, **20**, 3469–3472.
- 27 M. K. Reddy, I. Ramakrishna and M. Baidya, *Org. Lett.*, 2018, **20**, 4610–4613.
- 28 A. Yanagisawa, Y. Yamashita, C. Uchiyama, R. Nakano, M. Horiguchi and K. Ida, *Synlett*, 2019, **30**, 738–742.
- 29 B. M. Trost, J. S. Tracy and E. Y. Lin, *ACS Catal.*, 2019, **9**, 11082–11087.
- 30 T. Baumann, M. Bachle and S. Brase, *Org. Lett.*, 2006, **8**, 3797–3800.
- 31 T. Miura, M. Morimoto and M. Murakami, *Org. Lett.*, 2012, **14**, 5214–5217.
- 32 W. Yang, J. Sun, X. Xu, Q. Zhang and Q. Liu, *Chem. Commun.*, 2014, **50**, 4420–4422.
- 33 Y. Shen and G. K. Friestad, *J. Org. Chem.*, 2002, **67**, 6236–6239.
- 34 B. Zhou, J. Du, Y. Yang, H. Feng and Y. Li, *Org. Lett.*, 2014, **16**, 592–595.
- 35 X. Yan, X. Yang and C. Xi, *Catal. Sci. Technol.*, 2014, **4**, 4169–4177.
- 36 C. W. Kang, M. P. Sarnowski, Y. M. Elbatrawi and J. R. Del Valle, *J. Org. Chem.*, 2017, **82**, 1833–1841.
- 37 J. C. Monbaliu and J. Marchand-Brynaert, *Tetrahedron Lett.*, 2008, **49**, 1839–1842.

- 38 J. C. Monbaliu, B. Tinant and J. Marchand-Brynaert, *J. Org. Chem.*, 2010, **75**, 5478–5486.
- 39 B. S. Bodnar and M. J. Miller, *Angew. Chem., Int. Ed.*, 2011, **50**, 5630–5647.
- 40 T. A. Wencewicz, B. Yang, J. R. Rudloff, A. G. Oliver and M. J. Miller, *J. Med. Chem.*, 2011, **54**, 6843–6858.
- 41 S. Carosso and M. J. Miller, *Org. Biomol. Chem.*, 2014, **12**, 7445–7468.
- 42 B. Maji and H. Yamamoto, *J. Am. Chem. Soc.*, 2015, **137**, 15957–15963.
- 43 L. Brulíková, A. Harrison, M. J. Miller and J. Hlaváč, *Beilstein J. Org. Chem.*, 2016, **12**, 1949–1980.
- 44 M. G. Memeo and P. Quadrelli, *Chem. Rev.*, 2017, **117**, 2108–2200.
- 45 W. Adam and O. Krebs, *Chem. Rev.*, 2003, **103**, 4131–4146.
- 46 M. Baidya and H. Yamamoto, *Synthesis*, 2013, **45**, 1931–1938.
- 47 L. Zhai, X. Tian, C. Wang, Q. Cui, W. Li, S. H. Huang, Z. X. Yu and R. Hong, *Angew. Chem., Int. Ed.*, 2017, **56**, 11599–11603.
- 48 M. Baidya, K. A. Griffin and H. Yamamoto, *J. Am. Chem. Soc.*, 2012, **134**, 18566–18569.
- 49 K. Ohmatsu, Y. Ando, T. Nakashima and T. Ooi, *Chem.*, 2016, **1**, 802–810.
- 50 P. Merino, T. Tejero, I. Delso and R. Matute, *Synthesis*, 2016, **48**, 653–676.
- 51 I. Ramakrishna, V. Bhajammanavar, S. Mallik and M. Baidya, *Org. Lett.*, 2017, **19**, 516–519.
- 52 Y. A. Arbuzov and A. Markovskaya, *Bull. Acad. Sci. USSR, Div. Chem. Sci.*, 1952, **1**, 355–358.
- 53 N. J. Leonard, A. J. Playtis, F. Skoog and R. Y. Schmitz, *J. Am. Chem. Soc.*, 1971, **93**, 3056–3058.
- 54 O. Werbitzky, K. Klier and H. Felber, *Liebigs Ann. Chem.*, 1990, 267–270.
- 55 S. Ranganathan and K. S. George, *Tetrahedron*, 1997, **53**, 3347–3362.
- 56 A. Hall, P. D. Bailey, D. C. Rees, G. M. Rosair and R. H. Wightman, *J. Chem. Soc., Perkin Trans. 1*, 2000, 329–343.
- 57 W. Oppolzer and O. Tamura, *Tetrahedron Lett.*, 1990, **31**, 991–994.
- 58 W. Oppolzer, O. Tamura and J. Deerberg, *Helv. Chim. Acta*, 1992, **75**, 1965–1978.
- 59 W. Oppolzer, O. Tamura, G. Sundarababu and M. Signer, *J. Am. Chem. Soc.*, 1992, **114**, 5900–5902.
- 60 W. Oppolzer and E. Merifield, *Helv. Chim. Acta*, 1993, **76**, 957–962.
- 61 W. Oppolzer, P. Cintas-Moreno, O. Tamura and F. Cardinaux, *Helv. Chim. Acta*, 1993, **76**, 187–196.
- 62 W. Oppolzer, C. G. Jochet and E. Merifield, *Tetrahedron Lett.*, 1994, **35**, 7015–7018.
- 63 E. M. Stocking, R. A. Martinez, L. A. Silks, J. F. Sanz-Cervera and R. M. Williams, *J. Am. Chem. Soc.*, 2001, **123**, 3391–3392.
- 64 E. C. Davison, M. E. Fox, A. B. Holmes, S. D. Roughley, C. J. Smith, G. M. Williams, J. E. Davies, P. R. Raithby, J. P. Adams, I. T. Forbes, N. J. Press and M. J. Thompson, *J. Chem. Soc., Perkin Trans. 1*, 2002, **2**, 1494–1514.
- 65 N. A. Magnus, S. Campagna, P. N. Confalone, S. Savage, D. J. Meloni, R. E. Waltermire, R. G. Wethman and M. Yates, *Org. Process Res. Dev.*, 2010, **14**, 159–167.
- 66 B. Gutmann, D. Cantillo and C. O. Kappe, *Angew. Chem., Int. Ed.*, 2015, **54**, 6688–6728.
- 67 F. J. Strauss, D. Cantillo, J. Guerra and C. O. Kappe, *React. Chem. Eng.*, 2016, **1**, 472–476.
- 68 B. Gutmann and C. O. Kappe, *J. Flow Chem.*, 2017, **7**, 65–71.
- 69 M. Köckinger, C. A. Hone and C. O. Kappe, *Org. Lett.*, 2019, **21**, 5326–5330.
- 70 A. Steiner, J. D. Williams, O. De Frutos, J. A. Rincón, C. Mateos and C. O. Kappe, *Green Chem.*, 2020, **22**, 448–454.
- 71 A. Steiner, P. M. C. Roth, F. J. Strauss, G. Gauron, G. Tekautz, M. Winter, J. D. Williams and C. O. Kappe, *Org. Process Res. Dev.*, 2020, **24**, 2208–2216.
- 72 D. Dallinger, B. Gutmann and C. O. Kappe, *Acc. Chem. Res.*, 2020, **53**, 1330–1341.
- 73 R. Gérardy, M. Winter, A. Vizza and J.-C. M. Monbaliu, *React. Chem. Eng.*, 2017, **2**, 149–158.
- 74 R. Gérardy, N. Emmanuel, T. Toupy, V. Kassin, N. N. Tshibalanza, M. Schmitz and J.-C. M. Monbaliu, *Eur. J. Org. Chem.*, 2018, 2301–2351.
- 75 V. E. H. Kassin, R. Gérardy, T. Toupy, D. Collin, E. Salvadeo, F. Toussaint, K. Van Hecke and J.-C. M. Monbaliu, *Green Chem.*, 2019, **21**, 2952–2966.
- 76 N. Emmanuel, P. Bianchi, J. Legros and J.-C. M. Monbaliu, *Green Chem.*, 2020, **22**, 4105–4115.
- 77 V. E. H. Kassin, T. Toupy, G. Petit, P. Bianchi, E. Salvadeo and J.-C. M. Monbaliu, *J. Flow Chem.*, 2020, **10**, 167–179.
- 78 J.-C. M. Monbaliu, A. Cukalovic, J. Marchand-Brynaert and C. V. Stevens, *Tetrahedron Lett.*, 2010, **51**, 5830–5833.
- 79 J.-C. M. Monbaliu, L. K. Beagle, J. Kovacs, M. Zeller, C. V. Stevens and A. R. Katritzky, *RSC Adv.*, 2012, **2**, 8941–8945.
- 80 *Jaguar, version 8.5*, Schrodinger, Inc., New York, 2014.
- 81 M. J. Mintz and C. Walling, *Org. Synth. Coll.*, 1973, **5**, 183–187.
- 82 V. Dhayalan and P. Knochel, *Synthesis*, 2015, **47**, 3246–3256.
- 83 C. R. Johnson and J. J. Rigan, *J. Am. Chem. Soc.*, 1969, **91**, 5398–5399.
- 84 I. Sakai, N. Kawabe and M. Ohno, *Bull. Chem. Soc. Jpn.*, 1979, **52**, 3381–3383.
- 85 M. Pape, *Fortschr. Chem. Forsch.*, 1967, **7**, 559.
- 86 E. G. Bozzi, C.-Y. Shiue and L. B. Clapp, *J. Org. Chem.*, 1973, **38**, 56–59.
- 87 M. Kugelman, K. Mallams and F. Vernay, *J. Chem. Soc., Perkin Trans. 1*, 1976, 1113–1126.
- 88 R. Bou-Moreno, S. Luengo-Arratta, V. Pons and W. B. Motherwell, *Can. J. Chem.*, 2013, **91**, 6–12.
- 89 R. Bou-Moreno, S. Luengo-Arratta and W. B. Motherwell, *Tetrahedron Lett.*, 2011, **52**, 2097–2099.

- 90 E. Muller and H. Metzger, *Chem. Ber.*, 1954, **87**, 1282–1293.
- 91 E. Muller, H. Metzger and D. Fries, *Chem. Ber.*, 1954, **87**, 1449–1460.
- 92 C. Schenk and T. J. de Boer, *Recl.: J. R. Neth. Chem. Soc.*, 1979, **98**, 18–21.
- 93 D. Ranganathan, S. Ranganathan, C. B. Bao and K. Raman, *Tetrahedron*, 1981, **37**, 629–635.
- 94 B. C. Oxenrider and M. M. Rogic, *J. Org. Chem.*, 1982, **47**, 2629–2633.
- 95 M. Tordeux, K. Boumizane and C. Wakselman, *J. Fluor. Chem.*, 1995, **70**, 207–214.
- 96 A. K. Gupta, D. K. Dubey and M. P. Kaushik, *Org. Prep. Proced. Int.*, 2005, **37**, 294–298.
- 97 A. O. Terent'ev, I. B. Krylov, Y. N. Ogibin and G. I. Nikishin, *Synthesis*, 2006, 3819–3824.
- 98 V. Kumar and M. P. Kaushik, *Tetrahedron Lett.*, 2005, **46**, 8121–8123.
- 99 A. K. Gupta, J. Acharya, D. Pardasani and D. K. Dubey, *Tetrahedron Lett.*, 2007, **48**, 767–770.
- 100 R. A. Sheldon, *ACS Sustainable Chem. Eng.*, 2018, **6**, 32–48.
- 101 R. A. Sheldon, *Green Chem.*, 2017, **19**, 18–43.
- 102 H. Diekmann and W. Lüttke, *Angew. Chem., Int. Ed. Engl.*, 1968, **7**, 387–388.
- 103 A. H. A. Mohammed and G. Nagendrappa, *J. Chem. Sci.*, 2011, **123**, 433–441.
- 104 D. Prat, J. Hayler and A. Wells, *Green Chem.*, 2014, **16**, 4546–4551.
- 105 M. Ohno and I. Sakai, *Tetrahedron Lett.*, 1965, **50**, 4541–4544.
- 106 M. Ohno and N. Kawabe, *Tetrahedron*, 1966, **33**, 3935–3938.
- 107 S. Buscemi, A. Pace, A. P. Piccionello, G. Macaluso, N. Vivona, D. Spinelli and G. Giorgi, *J. Org. Chem.*, 2005, **70**, 3288–3291.
- 108 M. B. Plutschack, B. Pieber, K. Gilmore and P. H. Seeberger, *Chem. Rev.*, 2017, **117**, 11796–11893.
- 109 B. Picard, K. Pérez, T. Lebleu, D. Vuluga, F. Burel, D. C. Harrowven, I. Chataigner, J. Maddaluno and J. Legros, *J. Flow Chem.*, 2020, **10**, 139–143.
- 110 J. Andraos, *Reaction green metrics: problems, exercises, and solutions*, Taylor & Francis Group, LLC, 1st edn, 2018.
- 111 A. Armstrong, M. A. Atkin and S. Swallow, *Tetrahedron: Asymmetry*, 2001, **12**, 535–538.
- 112 D. M. Scarpino Schietroma, M. R. Monaco, V. Bucalossi, P. E. Walter, P. Gentili and M. Bella, *Org. Biomol. Chem.*, 2012, **10**, 4692–4695.
- 113 Y. Yamashita, H. Ishitani and S. Kobayashi, *Can. J. Chem.*, 2000, **78**, 666–672.
- 114 <http://ecoscale.cheminfo.org/calculator> (Accessed on January 28, 2021).
- 115 K. Van Aken, L. Streckowski and L. Patiny, *Beilstein J. Org. Chem.*, 2006, **2**, 1–7.